Dynamic Characteristics of Optical Intersecting-Waveguide Modulators/Switches with Curved Electrodes

Jamshid Nayyer, Kaveh Niayesh, and Minoru Yamada

***Abstract*—The dynamic behavior of optical modulators/switches in the form of intersecting waveguides with curved electrodes is formulated. It is shown that the electrode curvature is very effective in achieving reflected pulses in good resemblance to the incident ones. Further, the speed of operation is found to be high and is shown to depend, besides the commonly known capacitance of the device and the time required for refractive index variations to settle down, on the relative pulsewidths of the optical and modulating signals and the extent of their synchronization. The intersection angle is found to influence the propagation delays of the spatial components, which are equalized by properly chosen structural parameters, to achieve unbroadened and undistorted output pulses. The flexibility in the bandwidth of even a fabricated device, through adjustment of the driving conditions, is demonstrated and the capability of such devices to handle a very wide range of optical pulsewidths is clarified.**

***Index Terms*—Curved electrode, intersecting waveguides, modulating signal, optical signal, synchronization, temporal and spatial components.**

I. Introduction

EXTERNAL modulators and switches are important devices needed in high-speed optical communication systems. During the past decade, such systems have been introduced, to a large scale, in telecommunication networks where enormous bandwidths are attained over long haul trunk lines. Many research efforts have been spent in realization of fast modulators with low drive requirements and high quality optical switches for applications in routing of information carrying digital pulses. Among such investigations, semiconductor-based devices are promising candidates from the view point of the possibility of monolithic integration to high quality laser sources [1], [2]. Further, compound semiconductors in the form of quantum-wells are found to exhibit field-induced refractive index changes much larger than those realized in materials with large electrooptic coefficients such as $LiNbO_3$ [3], [4]. Based on such large refractive index variations, optical intersecting waveguide switches were proposed [5], [6] and their performance were investigated both theoretically and experimentally [7]–[13]. These research efforts showed that intersecting waveguide type optical switches/modulators with the possibility of monolithic integration to laser sources are small-size and small-loss devices with low drive requirements but sufficiently large extinction ratios are yet to be realized. As an improvement, the slightly curved electrode in the shape of an exponential spiral was proposed [14], [15]. It was shown that introduction of such spiral-form curvature brings about the possibility of realization of high-extinction ratios, low insertion-loss and small-size modulators/switches. This was achieved by adjusting the electrode curvature in the specific way to make it to pose a constant angle of incidence (within the critical angle) to all variously oriented plane-wave spatial components constituting the guided fundamental mode. Further, the electrode curvature was found to be useful in the reduction of frequency chirping and it was shown that the chirp behavior of a plane wave in reflection from a straight boundary is the same as that of a guided mode in reflection from a curved interface [16], [17]. Therefore, it was concluded that introduction of the electrode curvature is effective in improving the behavior of such optical modulator/switches. Although in real application of such devices, their dynamic behavior plays an important role, little is known about their pulse-operation characteristics and to the best knowledge of the authors, so far, there has been no report on this subject. It is commonly known that the speed of operation is limited by the capacitance of the device and the finite time required for the refractive index variations to settle down. However, the dynamic performance of such devices must thoroughly be understood if they are to be used in high-speed digital systems. Further, the pulse-handling capability is an important issue and such devices must operate under high bit rates. Presently, fast digital transoceanic communication systems with bandwidths of $\sim$10 Gb/s are in operation and future ones are expected to operate at about 100 Gb/s. Therefore, such devices must be capable of handling a few ps wide optical pulses. Besides high-speed optical communication systems, such devices can find various applications in the fields of precision instrumentation, lasers in medicine and surgery, machinery, etc., where the need arises frequently for laser pulses of specified shapes, widths and repetition rates. In these applications, the well-established pulse-shaping techniques (in electronics) can directly be employed to generate such desired optical pulses whereas their direct generation via laser sources may not be easy and mode-stability, frequency chirping, etc., are the problems that one is, usually, concerned with.

In this paper, the dynamic behavior of total internal reflection type optical modulators/switches in the form of intersecting

Manuscript received August 31, 1999; revised January 11, 2000.

J. Nayyer and M. Yamada are with the Department of Electrical and Computer Engineering, Faculty of Engineering, Kanazawa University, Kanazawa 920-8667, Japan.

K. Niayesh is with Institut fur Allgemaine Electrotechnik und Hochspannungtechnik, IHT RWTH, TH: Aachen 52056, Germany.

Publisher Item Identifier S 0733-8724(00)03736-1.

waveguides is formulated. The guided fundamental mode is expressed in terms of its spatial and temporal Fourier components and Snell's law is applied to investigate the reflected field variations. It is shown that introduction of the curved electrode is very effective in achieving reflected pulse forms in good resemblance to the incident ones. That the intersection-angle can be adjusted for equalization of propagation delays of the spatial components, is also shown which reduces the distortions associated with pulse operation. The device-speed is found to be sufficiently high for applications in wide band optical communication systems and shown to depend, besides the commonly known capacitance and the finite time required for refractive index changes to settle down, on the relative pulsewidths of the optical and modulating signals and the synchronization between them.

II. Analysis

An intersecting waveguide type external modulator/switch, shown in Fig. 1, is considered where two single-mode optical waveguides of width "a" intersect at angle "θ" and a curved electrode of (minimum) width "w" and length "l" is used for activation of the quantum-well material [14], [15]. In the interaction region, the quantum-well films [shown in Fig. 1(b)] are used. But, due to larger refractive index changes, quantum-well rods or dots might be preferred [18], [19]. When the modulating signal $V(t)$ is applied to the electrode, the incident mode undertakes total reflection at the boundary created under the electrode and propagates to the reflection port. The guided mode propagates directly to the transmission port if $V(t) = 0$.

In formulation of the dynamic behavior of the device, the field component of the guided mode is represented by

$$E_{\text{in}}(x, z, t) = F_r(x) g_{\text{in}}(t) \exp[-j\beta z] \tag{1}$$

where the confinement effect along y [see Fig. 1(b)] is taken care of by the well-known effective refractive index method. The problem reduces, therefore, to two intersecting slabs where $F_r(x)$ shows the transverse field distribution, $\exp[-j\beta z]$ stands for propagation along z and $g_{\text{in}}(t)$ represents the input time variations. At the input plane z_i, the field expressed in terms of its spectrum can be represented by

$$E_{\text{in}}(x, z_i, t) = (1/\sqrt{(2\pi)}) \int_{-\infty}^{\infty} F_r(x) \times \exp[-j\beta z_i] G_{\text{in}}(\omega_l) \exp[j\omega_l t]\, d\omega_l \tag{2}$$

where ω_l denotes the light central frequency. The transverse field distribution can, similarly, be expressed in terms of its plane-wave spatial components. Therefore

$$E_{\text{in}}(x, z_i, t) = (1/2\pi) \iint_{-\infty}^{\infty} F_f(k_x, \omega_l) G_{\text{in}}(\omega_l) \times \exp j[\omega_l t - \beta(\omega_l) z_i] \exp[-jk_x x]\, dk_x\, d\omega_l \tag{3}$$

where $F_f(k_x, \omega_l)$ denotes the spatial spectrum expressed by (4) in [7]. The dispersion effects are taken into consideration through frequency-variations represented by $\beta(\omega_l)$ and $F_f(k_x, \omega_l)$.

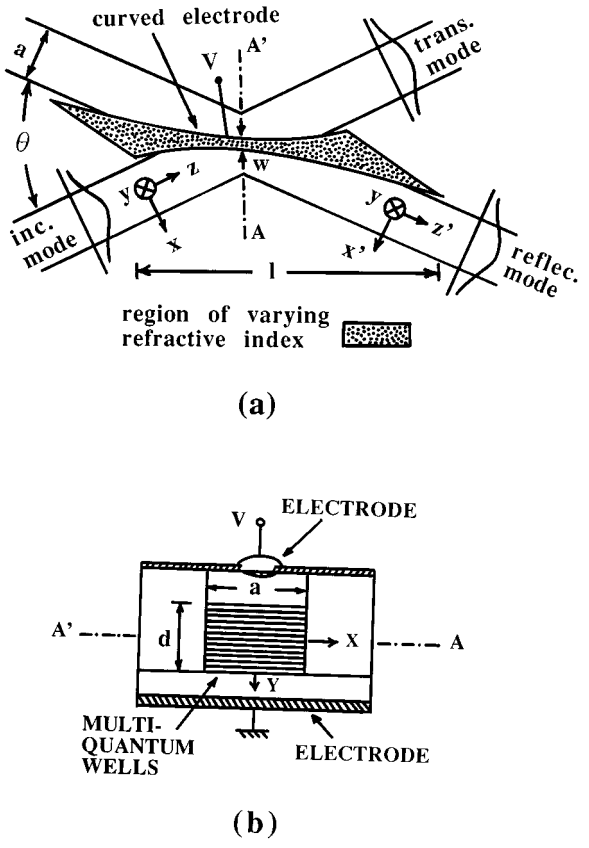

Fig. 1. Optical intersecting-waveguide type modulator/switch with curved electrode. (a) Top view and (b) cross section.

As shown in Fig. 2, each plane wave spatial component covers the distance $\rho(k_x)$ to reach the electrode where it is totally reflected. It further travels the distance $D_r(k_x)$ to the plane of observation at $z' = z_0$ [see also Fig. 1(a)]. Therefore, the output field distribution is

$$E_{\text{out}}(x', z_0, t) = (1/2\pi) \int_{K_1}^{K_2} \left\{ \int_{-\infty}^{\infty} F_f(k_x, \omega_l) r(k_x, t, \omega_l) \times \exp -j[\Psi_i(k_x, \omega_l) + \Psi_r(k_x, \omega_l)] G_{\text{in}}(\omega_l) \times \exp j[\omega_l t - \beta(\omega_l) z_i]\, d\omega_l \right\} \times \exp[-jk_{x'}(k_x) x']\, dk_x \tag{4}$$

where the reflection coefficient is denoted by $r(k_x, t, \omega_l)$ and the phase delays corresponding to propagation through distances ρ and D_r are represented by Ψ_i and Ψ_r, respectively, and $k_{x'}$ represents the reflected plane wave component along x' [15]. K_1 and K_2 denote the range of plane waves incident on the finite-length electrode [14]. If it is several hundred micrometers long, almost all plane wave components are captured and K_1, K_2 approach $-\infty$ and $+\infty$, respectively [20].

The dispersion effects must be taken into account for very narrow pulses on the order of tens of femtoseconds [21]. The

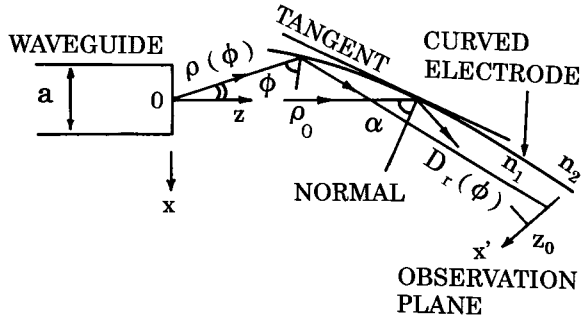

Fig. 2. Total reflection of plane-waves from the exponentially curved interface with equalized angles of incidence.

spectrum-width of a 10-fs Gaussian pulse generated by a mode locked laser is about 15% of its central frequency and, therefore, the reflection coefficient $r(k_x, t, \omega_l)$ is taken to vary with light frequency ω_l [5]. However, the dispersion effects can be ignored if picoseconds pulsewidths are dealt with. Under such circumstances (4) reduces to

$$E_{\text{out}}(x', z_0, t) = (1/2\pi) \int_{-\infty}^{\infty} r(k_x, t) s(k_x, t) \times \exp[-jk_{x'}(k_x)x'] \, dk_x \tag{5}$$

with

$$s(k_x, t) = F_f(k_x) \int_{-\infty}^{\infty} G_{\text{in}}(\omega_l) \times \exp j[\omega_l t - \Psi(k_x, \omega_l)] \, d\omega_l \tag{6}$$

and

$$\Psi(k_x, \omega_l) = \Psi_i(k_x, \omega_l) + \Psi_r(k_x, \omega_l) \tag{7}$$

where for the sake of convenience, the input plane is taken to be at $z_i = 0$. The output spectrum is given by

$$E_{\text{out}}(x', z_0, \omega_l) = (1/2\pi) \int_{-\infty}^{\infty} \exp[-jk_{x'}x'] R(k_x, \omega_s) * S(k_x, \omega_l) \, dk_x \tag{8}$$

where $*$ represents the convolution operation and $R(k_x, \omega_s), S(k_x, \omega_l)$ denote the Fourier transforms of $r(k_x, t)$ and $s(k_x, t)$, respectively, and ω_s shows the signal frequency. The light frequency spectrum is formed around the laser central frequency ω_l while that of the signal is in the vicinity of ω_s. In practice $\omega_l \gg \omega_s$ and in cases of very narrow pulsewidths where the dispersion effects can not be neglected, it is possible to ignore the very small overlap in the signal and optical tails of the time-dependent reflection coefficient $r(k_x, t, \omega_l)$. The phase delay in (7) is given by

$$\Psi(k_x, \omega_l) = \tau(k_x)\omega_l \tag{9}$$

with

$$\tau(k_x) = [\rho(k_x) + D_r(k_x)]n_1/c \tag{10}$$

where c and n_1 denote the light velocity and refractive index of the core and $\rho(k_x)$, $D_r(k_x)$ are determined in [15]. From (5), (6), (9) and (10), the output takes the form of

$$E_{\text{out}}(x', z_0, t) = (1/2\pi) \int_{-\infty}^{\infty} r(k_x, t) g_{\text{in}}(t + \tau(k_x)) \times F_f(k_x) \exp[-jk_{x'}x'] \, dk_x. \tag{11}$$

For a constant width exponentially curved electrode which poses a constant angle of incidence to all variously oriented plane wave spatial components, $r(k_x, t)$ becomes independent of k_x and can be taken out of the integral [14], [15]. In this regard, the previously proposed intersecting-curved-electrode configuration is helpful in reduction of the capacitance while maintaining the advantages of electrode curvature [22].

Further, it is possible, through proper choice of the structural parameters of the device, to equalize the delay times $\tau(k_x)$ of the plane wave spatial components (see Section III and Fig. 4). Therefore, (11) reduces to

$$E_{\text{out}}(x', z_0, t) = (1/2\pi) g_{\text{out}}(t) \int_{-\infty}^{\infty} F_f(k_x) \times \exp[-jk'_x x'] \, dk_x \tag{12}$$

with

$$g_{\text{out}}(t) = g_{\text{in}}(t + \tau) r(t). \tag{13}$$

As seen, the output pulse form is the product of the delayed input and the reflection coefficient which is very close to unity in the range of total reflection. It was previously shown that the spatial variations of the reflected output [expressed by the integral in (12)] is also improved as the consequence of introduction of the curved electrode. The improvement was manifested in terms of reduced Goos–Haenschen shift [15]. Therefore, the electrode curvature is said to be useful in improving the quality of both temporal and spatial variations of the reflected pulse forms.

The time dependent refractive index $n_2(t)$ of the material influenced by the electrode is expressed as

$$n_2(t) = (n_1 + \Delta n') + j(n'' + \Delta n'') \tag{14}$$

where the imaginary part stands for the absorption loss and the ratio of the real to imaginary changes, defined as the index-loss variation ratio, is shown by [8]

$$\alpha_p = \Delta n'/\Delta n''. \tag{15}$$

Then

$$n_2(t) = n_1[1 - (1 - \sqrt{(1 - 2\Delta_{\text{eq}})) f(t)}] + j[n'' + n_1(\sqrt{(1 - 2\Delta_{\text{eq}})} - 1) f(t)/\alpha_p] \tag{16}$$

where $f(t)$ shows the time variations of the signal and Δ_{eq} represents the perturbed relative refractive index difference. The

plane wave reflection coefficient of the three-layer structure is given by [23]

$$r(t) = [n_1^2 \cos^2\theta_2(t) - n_2^2(t)\cos^2\theta_1] \times (1 - e^{2jb})/\{[n_1\cos\theta_2(t) + n_2(t)\cos\theta_1]^2 - [n_1\cos\theta_2(t) - n_2(t)\cos\theta_1]^2 e^{2jb}\} \quad (17)$$

where b represents the normalized electrode width in the form of

$$b = 2\pi w n_2(t)\cos\theta_2(t)/\lambda \quad (18)$$

in which λ and w denote the wavelength and electrode-width and θ_1 shows the angle of incidence. θ_2 is related to θ_1 in the form of

$$\theta_2(t) = \cos^{-1}\{1 - [n_1\sin\theta_1/n_2(t)]^2\}^{1/2}. \quad (19)$$

III. Results

Following the analytical procedure shown in the previous section, numerical results on the dynamic behavior of intersecting waveguide modulators/switches with curved electrodes are to be presented. The structure shown in Fig. 1 is assumed to have the following parameters. The waveguide relative refractive index difference Δ_w is taken to be 0.1% with the normalized frequency of $V = 1$ (to ensure single mode operation). The voltage induced refractive index variation is taken to be $\Delta_{\text{eq}} = 1\%$ which is a realistic estimate of such changes in quantum-well structures [4], [18], [19]. This gives a critical (complementary) angle of 8.1° allowing the intersection-angle θ of up to 16.2°. However, a small marginal angle is required to ensure that the tunneling power can be neglected [25]. Therefore, as the widest-angle structure, θ is taken to be 14°. Further, such wide intersection angles ensure negligibly small coupling effects and help to avoid reflections at the interaction-region due to waveguide boundaries [26], [27]. As to the curved electrode, it is given by [14], [15]

$$\rho(\phi) = \rho_0 \exp[-C\phi] \quad (20)$$

where C is determined from the condition of total internal reflection [14]. The electrode curvature must sufficiently be small to give radius of curvature wave-number products on the order of 10^4 or even larger [25]. Further, $\rho_0 \gg a/2$ should be realized and larger radii of curvature result in more accurate analytical results [14]. On the other hand, scattering loss increases with ρ_0 and a proper choice was shown to be $\rho_0/(a/2) = 50$–70 [15]. Taking the waveguide width of $a = 5$–6 μm [see Fig. 1(a)], $\rho_0 = 100$–200 μm turn to be suitable values.

Fig. 3 shows typical reflected pulse forms where the optical and modulating signals $g_{\text{in}}(t)$ and $f(t)$ are both taken to be Gaussian with pulsewidths shown by t_o and t_s, respectively. t_s is limited by capabilities of the electronic circuitry. Further, when the main component spatial plane wave ρ_0 (along z axis) impinges on the electrode, the modulating signal must have been applied slightly earlier and has to be sustained a little later to allow for reflection of the nearest and farthest components.

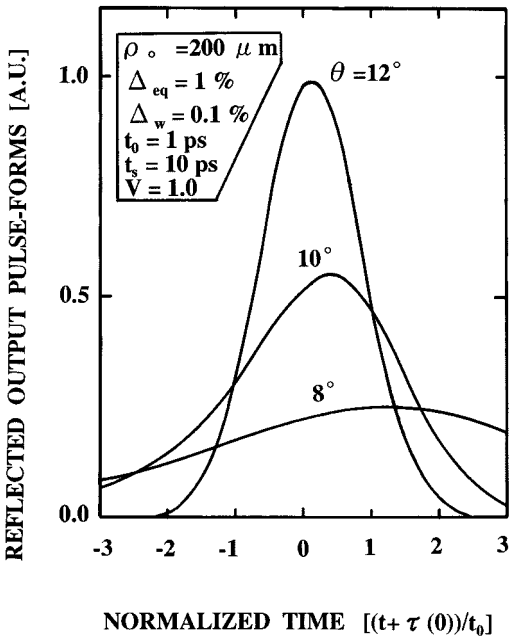

Fig. 3. Time-display of reflected pulses.

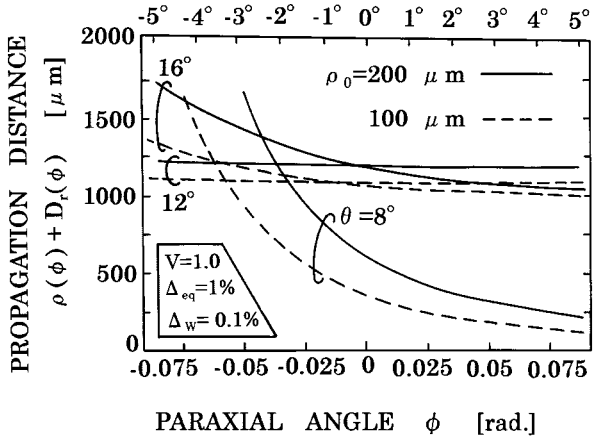

Fig. 4. Propagation distances of plane-wave components versus their angle with respect to direction of propagation.

Their delay difference is a few ps inside the core material of refractive index $n_1 \sim 3.5$. Therefore, t_s is taken to be 10 ps while t_0 is assumed to be 10 times narrower ($t_o = 1$ ps) where the dispersion effects can still be neglected. The horizontal axis shows the normalized time $(t+\tau(0))/t_o$ where $\tau(0)$ denotes the delay time of the main component expressed in (10) and the angle of intersection θ is taken as the parameter. It is seen that as θ is increased, the output pulse form is improved and at $\theta = 12°$ quite narrow output pulses (a few picoseconds widths) are achievable. That is, the device can serve as an external modulator or a switch in high bit rate (~100 Gb/s) digital optical communication systems. Further wider intersection angles (still within the critical angle) were also treated but the corresponding pulsewidths were found to be larger which are, however, to be avoided because of limitations described earlier. To interpret this interesting result, the plane-wave time delays are investigated, as shown in Fig. 4, where θ is taken again as the parameter. As seen, at both values of ρ_0, the propagation distances $\rho + D_r$ are equalized at $\theta \sim 12°$

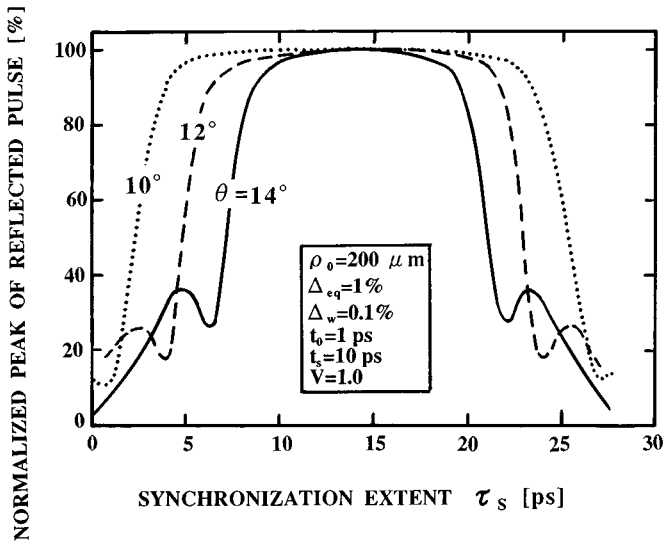

Fig. 5. Output pulse-peaks versus the extent of synchronization between optical and modulating signals.

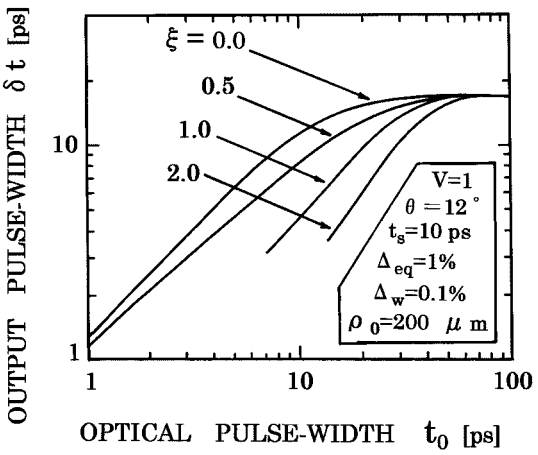

Fig. 6. Reflected pulsewidths versus optical pulsewidths.

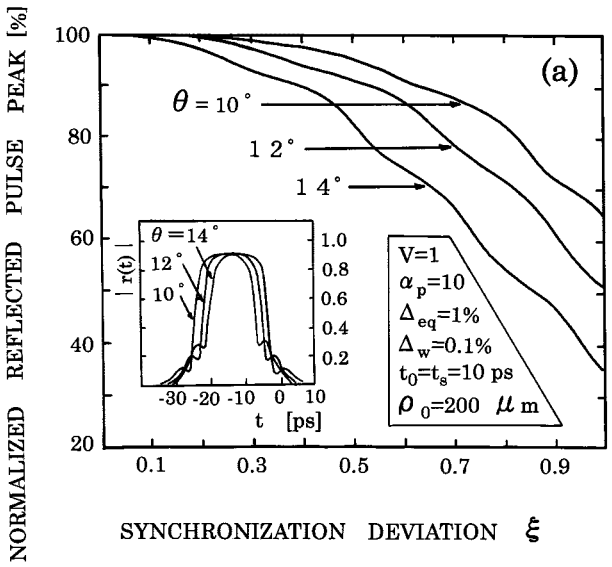

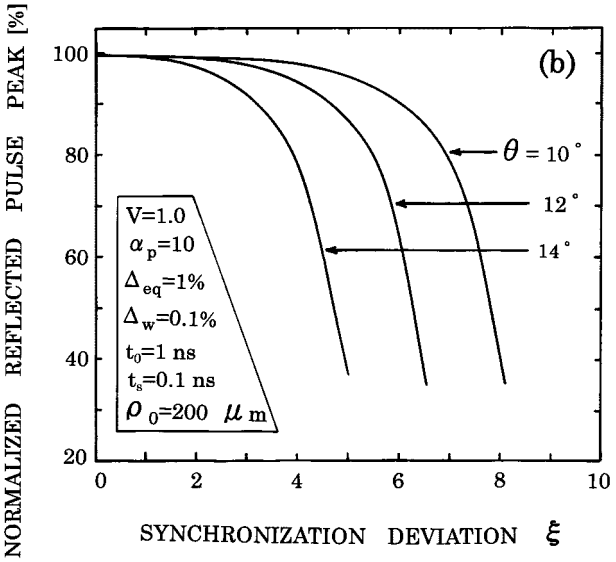

Fig. 7. Output pulse-peaks versus synchronization-deviations. (a)—narrow pulses of $t_o = t_s = 10$ ps. (b)—wide pulses of $t_o = 1$ ns, $t_s = 0.1$ ns.

while they are remarkably dispersed at smaller and larger intersection angles. That is, by the suitable choice of structural parameters, it is possible to adjust the plane-wave delays such that they all feel the region of maximum time dependent reflection coefficient through delayed (i.e., properly synchronized) modulating signal applied to the electrode. In this way, the extent of synchronization between the modulating and optical signals leaves a remarkable influence on the reflected pulse.

Fig. 5 shows the reflected pulse peak versus the required delay τ_s applied to the modulating signal of the form $\exp[-(t-\tau_s)^2/t_s^2]$ and the intersection angle θ as the parameter. At each θ, the pulse peaks are normalized to the maximum achievable one. As seen, maximum reflected output could be achieved if the modulating signal is properly delayed. In this respect, there is a wider range of synchronization τ_s in smaller interaction angles (i.e., $\theta = 10°$) which shrinks when θ is increased. The output pulse peak drops off very quickly once the optical and modulating signals fall out of synchronism.

Fig. 6 shows the output pulsewidth δt versus the optical pulsewidth t_o where deviations from synchronization defined as $\xi = (\tau(0) - \tau_s)/\tau(0)$ is taken as the parameter. As seen, the output pulsewidth δt increases almost linearly with the optical pulsewidth t_o and saturates at large t_o where it is solely determined by the modulating pulsewidth t_s. Further, the output pulsewidth δt is influenced by the synchronization deviations ξ which results in a flexible operation-speed of even a fabricated device. That is, it becomes possible to achieve reflected pulses of different widths by simply controlling the extent of synchronization deviations which brings about a 2–3 times flexibility in the pulsewidth handling capability of the device. At large synchronization deviations ($\xi = 1.0$ and 2.0), the output pulse form is distorted and the corresponding data are not presented in the region where double peaks have appeared. In such cases which result in erroneous data in digital communications, the pulsewidth cannot be defined uniquely and, therefore, representation of the output pulsewidth is avoided. There is, therefore, a tradeoff between the flexibility in speed of operation and the distortionless reflection of the

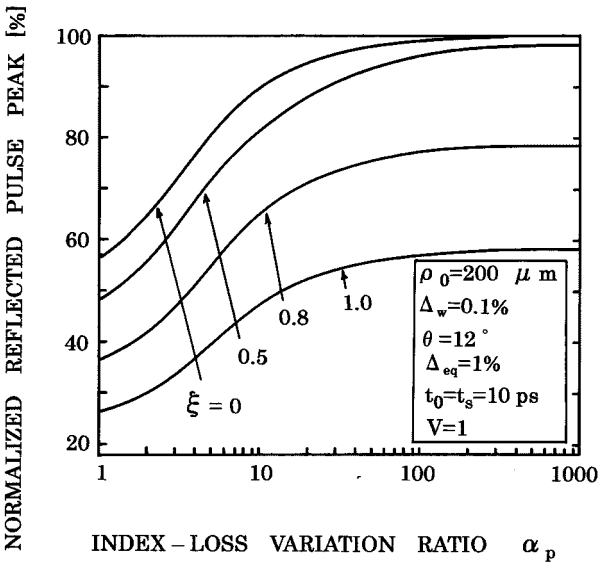

Fig. 8. Effects of absorption-loss on output pulse-peaks.

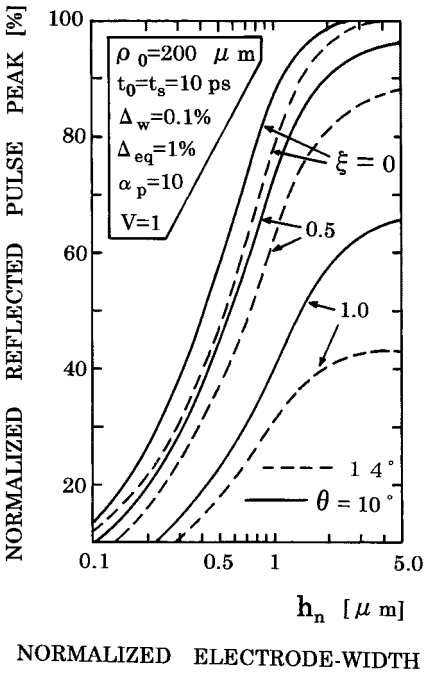

Fig. 9. Reflected pulse-peaks versus electrode-width.

incident pulse. Besides the output pulsewidth, its peak is also influenced by synchronization deviations ξ, as shown in Fig. 7 where the intersection angle is taken as the parameter. As seen in Fig. 7(a) where narrow 10 ps width Gaussian pulses are treated, the wider the intersection-angle, the more vulnerable the device is to synchronization deviations. This is due to the fact that, as the angle of intersection is increased, the time-dependent reflection coefficient $r(t)$ becomes narrower as shown inside this figure. Therefore, there is a shorter range of synchronization deviations over which large reflected pulse peaks could be sustained. In order to show the wide range of the pulse-handling capabilities of the device, the modulating signal is taken to be $t_s = 0.1$ ns in Fig. 7(b) which can easily be supplied via planar metallic waveguides. On the other hand, wide optical pulses of $t_o = 1$ ns are assumed. As seen, the output peak drops off very quickly with increasing synchronization deviation ξ. Such rapid decrease can be interpreted taking the point into consideration that since $t_o \gg t_s$, the output is determined mainly by the shape of reflection coefficient $|r(t)|$ [look at it inside Fig. 7(a)]. Wider optical pulses were also treated and the results followed similar trends. That is, the pulse-peak was seen to drop off with increasing ξ while its width was determined by that of the modulating signal. The significance of synchronization deviation was, however, seen to be lost if dc laser outputs are fed into the device. This demonstrates the wide range of pulsewidths which can be handled by such intersecting-waveguide type devices and justifies their applications in precision instrumentation, surgeries and medical treatments by lasers, etc., as mentioned earlier.

It is known that absorption-loss changes associated with refractive index variations degrade the modulation/switching characteristics of the device [8], [9]. Its influences on the dynamic behavior are investigated with the results depicted in Fig. 8 where the reflected pulse peak (normalized to its maximum) is plotted against α_p and ξ is taken as the parameter. At no synchronization deviation (i.e. $\xi = 0$), 90% of the output can be obtained at $\alpha_p > 10$. In this respect, there are, fortunately, wavelengths where such large α_p can be realized in quantum rods and dots [9]. The curves in this figure can serve to distinguish between the losses due to absorption and those caused by synchronization deviations. As stated earlier, the latter may be slightly introduced, through adjustment of the drive conditions, to achieve faster operation.

The electrode width leaves drastic effects on the device operation-speed. It must be narrow to ensure small capacitance while it has to be wide enough to let the total reflection to take place. Fig. 9 shows the output pulse peak (normalized with that at $\alpha_p = 10, \xi = 0$ and $h_n = \infty$) versus the normalized electrode width h_n ($=2w/\lambda$ with w representing the electrode-width) and ξ, θ taken as parameters. As seen, the output increases with increasing electrode width and similar trends are observed at various synchronization deviations ξ and intersection angles θ. In the design of such curved electrodes, a minimum width slightly larger than the wavelength suffices to maintain high quality reflections at the boundary.

IV. Conclusion

Formulation of the dynamic behavior of optical modulator/switches in the form of intersecting waveguides with curved electrodes was carried out through expression of the guided mode in terms of its temporal and spatial Fourier components. It was shown that the electrode curvature is very useful in achieving reflected pulses as good replica of the incident ones. The possibility of several hundred giga-Hertz operation of the device was predicted justifying their application in high-speed digital communication systems. The operation-speed was shown to depend, besides the commonly known capacitance and the time required in refractive index variations to settle down, on the relative pulsewidths of the

optical and modulating signals and the extent of their synchronization. The possibility of adjustment of the structural parameters in achieving equalized propagation delays resulting in unbroadened and undistorted output pulses was also shown. It was found that the operation-speed of even a fabricated device could be varied 2–3 times by controlling only the drive conditions.

REFERENCES

[1] Y. Suematsu and S. Arai, "Integrated optics approach for advanced semiconductor lasers," *Proc. IEEE*, vol. 75, pp. 1472–1487, Nov. 1987.

[2] R. C. Alferness, "Waveguide electrooptic switch arrays," *IEEE J. Select. Areas Commun.*, vol. 6, pp. 1117–1130, Aug. 1988.

[3] H. Yamamoto, M. Asada, and Y. Suematsu, "Electric field induced refractive-index variation in quantum-well structure," *Electron. Lett.*, vol. 21, pp. 579–580, June 1985.

[4] T. H. Wood, R. W. Tkach, and A. R. Charaplyvy, "Observation of large quadratic electro-optic effect in GaAs/AlGaAS multiple quantum wells," *Appl. Phys. Lett.*, vol. 50, pp. 798–800, Mar. 1987.

[5] H. Yamamoto, M. Asada, and Y. Suematsu, "Intersectional waveguide type optical switch with quantum well structure," *IEICE Trans. Japan*, vol. E-68, pp. 737–739, Nov. 1985.

[6] ——, "Theory of refractive index variation in quantum-well structure and related intersectional optical switch," *J. Lightwave Technol.*, vol. 6, pp. 1831–1840, Dec. 1988.

[7] J. Nayyer, Y. Suematsu, and K. Shimomura, "Analysis of reflection-type optical switches with intersecting waveguides," *J. Lightwave Technol.*, vol. 6, pp. 1146–1152, June 1988.

[8] K. Shimomura, Y. Suematsu, and S. Arai, "Analysis of semiconductor intersectional waveguide optical switch-modulator," *IEEE J. Quantum Electron.*, vol. 26, pp. 883–891, May 1990.

[9] ——, "Operational wavelength range of GaInAs(P)-InP intersectional optical switches using field-induced electrooptic effect in low-dimensional quantum-well structures," *IEEE J. Quantum Electron.*, vol. 28, pp. 471–477, Feb. 1992.

[10] T. Kikugawa, K. G. Ravikumar, K. Shimomura, A. Izumi, M. Matsubara, Y. Miyamoto, S. Arai, and Y. Suematsu, "Switching operation in OMVPE grown GaInAs/InP MQW intersectional optical switch structures," *IEEE Photon. Technol. Lett.*, pp. 126–128, June 1989.

[11] J. E. Zucker, K. L. Jones, G. R. Jacobovitz, B. Tell, K. Brown-Goebeler, T. Y. Chang, N. J. Sauer, M. D. Divino, M. Wegener, and D. S. Chemla, "InGaAs/InAlAs quantum well intersecting waveguide switch operating at 1.55 μm," *IEEE Photon. Technol. Lett.*, vol. 2, pp. 804–806, Nov. 1990.

[12] K. G. Ravikumar, K. Shimomura, T. Kikugawa, A. Izumi, K. Matsubara, S. Arai, and Y. Suematsu, "GaInAsP/InP MQW intersectional optical switch/modulator using field induced refractive index variation," *IEICE Trans. Japan*, vol. E-72, pp. 384–391, Apr. 1989.

[13] C. Z. Zhao, A. H. Chen, E. K. Liu, and G. Z. Li, "Silicon-on-insulator asymmetric optical switch based on total internal reflection," *IEEE Photon. Technol. Lett.*, vol. 9, pp. 1113–1115, Aug. 1997.

[14] J. Nayyer, H. Hatami-Hanza, and S. Safavi-Naeini, "Optical intersecting waveguide switches with curved electrodes," *IEICE Trans. Electron.*, vol. E77-C, pp. 69–76, Jan. 1994.

[15] ——, "Extinction ratios and scattering losses of optical intersecting waveguide switches with curved electrodes," *J. Lightwave Technol.*, vol. 12, pp. 1475–1481, Aug. 1994.

[16] J. Nayyer, K. Niayesh, S. Safavi-Naeini, and K. Komori, "Chirp improvement of optical intersecting waveguide switch/modulators by electrode curvature," *IEEE Photon. Technol. Lett.*, vol. 9, pp. 1586–1588, Dec. 1997.

[17] J. Nayyer, K. Niayesh, and S. Safavi-Naeini, "Application of slightly curved exponential interfaces in chirp reduction of optoelectronic devices and integrated circuits," in *Proc. Tech. Dig. First Optoelectron. Commun. Conf. (OECC'96)*, July 16–19, 1996, Paper 18P–21, pp. 462–463.

[18] K. G. Ravikumar, T. Aizawa, K. Matsubara, M. Asada, and Y. Suematsu, "Analysis of electric field effect in quantum box structure and its application to low loss intersectional type optical switch," *J. Lightwave Technol.*, vol. 9, pp. 1376–1385, Oct. 1991.

[19] T. Aizawa, K. Shimomura, S. Arai, and Y. Suematsu, "Observation of field induced refractive index variation in quantum box structure," *IEEE Photon. Technol. Lett.*, vol. 3, pp. 907–909, Oct. 1991.

[20] J. Nayyer and S. Safavi-Naeini, "Characteristics of reflection type switches with intersecting waveguides—Electrode length dependency," *IEICE Trans. of Japan*, vol. E-73, pp. 195–197, Feb. 1990.

[21] Ch. Spielmann, P. F. Curley, T. Barbee, E. Winter, and F. Krausz, "Generation of sub-20 fs mode locked pulses from Ti:sapphire laser," *Electron. Lett.*, vol. 28, pp. 1532–1534, July 30, 1992.

[22] K. Niayesh, J. Nayyer, A. Shooshtari, and S. Safavi-Naeini, "Speed-increase of optical switch/modulators by intersecting curved electrodes," in *Proc. Tech. Dig. Second Optoelectron. Commun. Conf. (OECC'97)*, July 8–11, 1997, Paper 8B2–4, pp. 36–37.

[23] M. Born and E. Wolf, *Principles of Optics*, 6 ed. London, U.K.: Pergamon, 1989, pp. 61–70. with corrections.

[24] J. E. Zucker, T. L. Hendrickson, and C. A. Burrus, "Low voltage phase modulation in GaAs/AlGaAs quantum well waveguides," *Electron. Lett.*, vol. 24, pp. 112–113, Jan. 1988.

[25] A. W. Snyder and J. D. Love, "Reflection at a curved dielectric interface—Electromagnetic tunneling," *IEEE Trans. Microwave Theory Tech.*, vol. MT-23, pp. 134–141, Jan. 1975.

[26] W. Mevenkamp, "Modeling and BPM calculation of electrooptic devices on $LiNbO_3$," *Integr. Optic. Circuit Eng. III*, vol. 651, pp. 162–168, 1986.

[27] A. Neyer, W. Mevenkamp, and J. Ctyroky, "Single-mode Ti:$LiNbO_3$ waveguide crossing and switches: Design rules and applications," *Integr. Optic. Circuit Eng. III*, vol. 651, pp. 169–176, 1986.

Jamshid Nayyer received the B.S. and M.S. degrees from Shiraz University, Shiraz, Iran, and the Ph.D. degree from the Tokyo Institute of Technology, Tokyo, Japan, all in electronics engineering in 1968, 1971, and 1976, respectively.

From September 1986 to September 1987, he was a Visiting Scholar at the Tokyo Institute of Technology. He joined the Central Opto-Electronics Research Labs. of Sumitomo Cement Company, in January 1991, where he was involved in the research and development of fast optical modulators. In March 1997, he was assigned to the Electro-technical Laboratory of the Ministry of International Trade and Industry (MITI), where he carried out research on ultrafast optical passive devices until March 1999. Since April 1999, he has been the Associate Professor in the Department of Electrical and Computer Engineering, Kanazawa University, Japan. His research interests are in optical devices and communication systems.

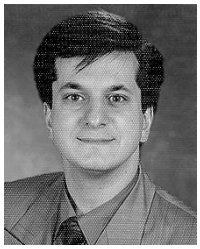

Kaveh Niayesh was born in Tehran, Iran, in 1971. He received the B.Sc. and M.Sc. degrees in electrical engineering from the University of Tehran in 1993 and 1996, respectively. He is currently pursuing the Ph.D. degree in electrical engineering at the Aachen University of Technology (RWTH-Aachen), Germany.

Minoru Yamada was born in Yamanashi, Japan, on January 26, 1949. He received the B.S. degree in electrical engineering from Kanazawa University, Kanazawa, Japan, in 1971 and the M.S. and Ph.D. degrees in electronics engineering from the Tokyo Institute of Technology, Tokyo, Japan, in 1973 and 1976, respectively.

In 1976, he joined Kanazawa University, where he is presently a Professor. From 1982 to 1983, he was a Visiting Scientist at Bell Laboratories, Holmdel, NJ. He is currently doing research work on semiconductor injection lasers, semiconductor optical switches and unidirectional optical amplifiers.

Dr. Yamada received the Yonezawa Memorial Prize in 1975, the Paper Award in 1976 and the Achievement Award in 1978 from the Institute of Electronics and Communication Engineers of Japan.